ARTICLE IN PRESS

Available online at www.sciencedirect.com

SCIENCE DIRECT®

Chemical Physics xxx (2006) xxx–xxx

Chemical Physics

www.elsevier.com/locate/chemphys

Computational study of neutral and cationic pericondensed polycyclic aromatic hydrocarbons

Amit Pathak, Shantanu Rastogi *

Department of Physics, D.D.U. Gorakhpur University, Gorakhpur 273 009, India

Received 29 October 2005; accepted 10 February 2006

Abstract

Quantum chemical calculations using density functional theory are presented for small to medium sized pericondensed PAHs including some being reported for the first time. Bond lengths and charge distribution have been computed for these PAHs in both neutral and cationic forms. Upon ionization, significant change in fractional charge on atoms is present particularly for the outer carbon atoms. The charge on the internal carbon atoms tends towards zero in cations. Vibrational frequencies and infrared intensities have been calculated for the optimized structures of PAH neutrals and cations. The drastic intensity alterations occurring upon ionization are discussed and related to specific changes occurring in the charge distribution. The C–H stretch intensity depends on the partial charge on peripheral hydrogen atoms and reduces in cations as hydrogen atoms become more positive. Pericondensed PAHs show better matching with the observed interstellar infrared bands. The co-added model spectra show profiles similar to the observed astrophysical bands.

Keywords: PAH; IR spectra; Aromatic infrared bands; Interstellar molecules; DFT; Charge distribution

1. Introduction

The spectra from diverse astrophysical objects such as HII regions, planetary nebulae, reflection nebulae, post AGB stars, star forming regions, interstellar medium (ISM) of our galaxy and that of outer galaxies show the presence of aromatic infrared bands (AIBs) centred at 3.3, 6.2, 7.7, 8.6, 11.2 and 12.7 μm (3030, 1610, 1300, 1160, 890 and 785 cm^{-1}) [1–4] with intensity and band profile variations from source to source [4–7]. These bands are spectral signatures attributed to polycyclic aromatic hydrocarbon (PAH) molecules [8–11]. The ubiquitous presence of AIBs makes PAHs important component of the molecular universe and are also considered as possible contributors to the UV extinction curve [12,13] and the diffuse interstellar bands (DIBs) [14–16].

PAHs have planar structure of fused benzenoid rings with the π electrons delocalized over the whole carbon skeleton providing high photo-stability and a large surface area for efficient absorption of background radiations. Absorption of a single UV photon results in vibrational heating of the PAH up to temperatures of nearly 1000 K. The isolated molecule de-excites through infrared emissions [10,11]. For a better understanding and identification of the carriers of interstellar AIB features, a widespread effort is being put to measure and calculate the vibrational properties of PAHs [5,17–33]. Strong UV radiations from background stars may also result in ionization of PAHs which complicates the analysis of the resulting composite spectra. The band positions for ionized PAHs differ little from neutrals but there is a remarkable difference in the intensity patterns [20–29].

The understanding of the IR spectra of PAHs and its variations with size and ionization state is needed to analyse the AIB features from various astrophysical environments. With this view and in continuation of the earlier report on catacondensed PAHs [23], we present here study of some pericondensed PAHs. Pericondensed PAHs are more compact and stable compared to linear PAHs. Studies related to photo-physical stability of PAHs in harsh environments have concluded that PAHs in the ISM must

* Corresponding author. Tel.: 915512204517; fax: +915512330767.
E-mail address: shantanu_r@hotmail.com (S. Rastogi).

0301-0104/$ - see front matter © 2006 Published by Elsevier B.V.
doi:10.1016/j.chemphys.2006.02.008

4-31G basis set are well established [21–23] and need a single scale factor to bring the vibrational frequencies in conjunction with the experimental data [21,23,40] but results in an overestimation of the C–H stretch intensity in the case of neutral molecules. The use of larger basis sets 6-31G or 6-31G** give comparatively better C–H stretch intensity match with experiments [21,23,40], but computational time increases many-folds and the scaling procedure also gets complicated [41,42]. Therefore, the use of larger basis sets is avoided.

Mulliken population analysis, which is based on wavefunction partitioning in terms of basis functions, is used to study the charge distribution. The method is most useful for comparing trends in electron distributions when small or medium sized basis sets are used [43]. The analysis is thus useful in the study of variations from neutrals to cations.

The calculated frequencies for some smaller PAHs, naphthalene, anthracene and pyrene, were compared with the reported matrix isolation spectra to obtain the best fit scale factor of 0.956. The calculated frequencies of all studied PAHs [23] are scaled by this factor and a good correlation with the reported experimental data, wherever available, is obtained. The calculated spectra have been plotted considering Gaussian profiles with full width half maximum to be 30 cm^{-1}, which is the typical width for PAHs emitting in conditions present in the ISM [10].

3. Results

The spectra of PAH cations are remarkably different from their neutral counterparts in terms of intensities of major peaks [5,17–33]. The spectra of neutrals are dominated by C–H stretch and C–H out of plane bend modes, whereas in cations the intensity of C–H in plane bend and C–C stretch modes (1150–1600 cm^{-1}) are increased by an order of magnitude and the C–H stretch mode intensity is drastically reduced by a similar factor. The C–H out of plane bend mode remains unaffected and has similar intensity in both neutrals and cations. The variations in intensities are attributed to the changes occurring in the charge distribution upon ionization of the molecules as in the case of catacondensed PAHs [23]. In order to pinpoint these changes and to relate them to the variations in the infrared intensities, the charge distribution of studied pericondensed PAHs is presented in Table 1; wherein comparisons for neutrals and cations are shown only for atoms where there is significant change.

Ionization induces small changes as far as the structure of the molecule is concerned with no or little change in bond lengths. To gain insight into structural changes induced by ionization, bond lengths for bonds showing large change are also presented in Table 1. The symmetry of the molecules is preserved in the ionized species except for highly symmetric molecules viz. triphenylene (D_{3h}) and coronene (D_{6h}), which show reduced symmetry upon ionization. It seems that, as a consequence of Jahn–Teller

Table 1
Bond length and charge distribution of studied PAHs

Bond Lengths			Charge distribution		
Bonds[a]	Neutral	Cation	Atoms[a]	Neutral	Cation
Pyrene					
b	1.403	1.423	C1	−0.122	−0.114
c	1.437	1.417	C2	−0.159	−0.101
e	1.360	1.384	C4	−0.138	−0.113
f	1.427	1.417	H6	0.127	0.191
			H7	0.127	0.192
			H8	0.128	0.189
Triphenylene					
f	1.423	1.453	C1	−0.123	−0.101
k	1.413	1.433	C2	−0.144	−0.119
l	1.465	1.428	C4	0.008	0.043
			C7	−0.123	−0.087
			C9	−0.144	−0.107
			H10	0.127	0.184
			H11	0.132	0.176
			H12	0.132	0.176
			H13	0.127	0.191
			H14	0.127	0.187
			H15	0.132	0.179
Perylene					
a	1.374	1.387	C1	−0.139	−0.104
c	1.405	1.392	C2	−0.125	−0.114
e	1.391	1.412	C3	−0.155	−0.111
f	1.475	1.451	H7	0.128	0.184
			H8	0.128	0.183
			H9	0.130	0.175
Benzo(e)pyrene					
d	1.424	1.445	C1	−0.123	−0.114
e	1.467	1.448	C2	−0.149	−0.098
f	1.402	1.421	C4	0.013	0.029
l	1.434	1.414	C5	−0.144	−0.129
m	1.358	1.381	C6	−0.123	−0.105
n	1.404	1.421	C7	−0.151	−0.100
			C9	−0.139	−0.117
			H11	0.127	0.185
			H12	0.131	0.183
			H13	0.132	0.166
			H14	0.127	0.178
			H15	0.127	0.186
			H16	0.129	0.187
Anthanthrene					
c	1.396	1.415	C1	−0.151	−0.113
e	1.442	1.429	C3	−0.164	−0.116
f	1.357	1.370	C5	−0.135	−0.117
g	1.443	1.429	C6	−0.135	−0.118
i	1.384	1.405	C8	−0.198	−0.144
			H12	0.127	0.179
			H13	0.128	0.181
			H14	0.127	0.181
			H15	0.129	0.177
			H16	0.129	0.176
			H17	0.128	0.181
Coronene					
b	1.423	1.435	C1	−0.145	−0.134
c	1.371	1.394	C2	−0.145	−0.108
d	1.423	1.406	C3	−0.145	−0.126
f	1.423	1.440	C5	0.047	0.074
			H8	0.129	0.176
			H9	0.129	0.179
			H10	0.129	0.181

(continued on next page)

Table 2
Comparison of IR frequencies (cm^{-1}) and relative intensities for benzo(e)pyrene[a]

Neutral					Cation				
Computed result			Experimental result[b]		Computed result			Experimental result[c]	
	Freq. (cm^{-1})	Rel. int.	Freq. (cm^{-1})	Rel. int.		Freq. (cm^{-1})	Rel. int.	Freq. (cm^{-1})	Rel. int.
B_2	549.8	0.05	554.5	0.05	B_2	628.8	0.06		
B_1	567.6	0.06	570.6	0.07	B_1	676.1	0.11	685.7	0.15
B_2	634.8	0.03	645.9	0.02	A_2	692.7	0.06		
B_1	701.9	0.09	711.8	0.18	A_2	751.1	0.09		
B_1	752.7	1.00	750.0	1.00	B_1	760.1	0.47		
			771.1	0.15	B_1	852.9	0.25	848.0	0.22
B_1	833.8	0.67	830.1	0.51	B_2	861.9	0.11	873.3	0.13
			842.9	0.14	A_2	935.4	0.06		
B_1	896.5	0.09	898.2	0.03	A_2	978.5	0.13		
B_2	1033.6	0.03	1037.8	0.04	B_2	1166.0	0.05		
A_2	1110.1	0.03	1106.9	0.04	A_2	1206.9	0.34	1193.9	0.21
B_2	1207.4	0.04	1191.8	0.09	B_2	1215.9	0.08		
A_2	1311.6	0.05	1320.6	0.07	A_2	1272.1	0.27	1264.3	0.14
B_2	1317.2	0.04			A_2	1294.3	0.43	1308.2	0.19
A_2	1399.3	0.15	1413.5	0.20	B_2	1299.1	0.78		
B_2	1432.5	0.09	1444.1	0.19	B_2	1319.2	0.47	1336.0	0.81
B_2	1460.9	0.17	1478.9	0.08				1349.2	1.00
B_2	1504.7	0.07			B_2	1335.6	0.16	1357.0	0.15
A_2	1584.9	0.15	1593.2	0.03	A_2	1338.9	0.07		
A_2	3031.5	0.05	3018.0	–	B_2	1386.0	0.17	1368.2	0.13
B_2	3049.8	0.41	3036.0	–	A_2	1405.8	0.15	1410.5	0.41
B_2	3051.9	0.13	3059.7	1.23	B_2	1430.9	0.12	1435.6	0.09
B_2	3064.5	0.32		–	B_2	1526.2	1.00	1556.8	0.88
A_2	3067.8	0.23		–	B_2	1538.4	0.08		
B_2	3068.3	0.35		–	A_2	1540.5	0.07		
A_2	3085.1	0.46		–	B_2	1579.2	0.14		
A_2	3103.1	0.48	3091.0	–	B_2	3073.2	0.04		
B_2	3105.9	0.13	3108.7	–	A_2	3122.4	0.06		

Max. absolute int. Neutral – 2.32 $Debye^2/amu\ Å^2$; cation – 5.42 $Debye^2/amu\ Å^2$.
[a] Irreducible representations are given for each normal mode.
[b] Ref. [31].
[c] Ref. [32].

data for both neutral and cation (Table 2). Two trio and one quartet group of hydrogens contribute to the most intense peak at 752 cm^{-1}, while the peak at 833.8 cm^{-1} is due to the duo hydrogens in the spectra of neutral benzo(e)pyrene (Fig. 3). Because of lower symmetry of this molecule, the C–H stretch mode intensity is divided amongst several moderate peaks, which seem to merge in the plot using FWHM of 30 cm^{-1}. Spectra of cation shows similar C–H out of plane bend features as in the neutral species. The most intense feature at 1300 cm^{-1} is an overlap of neighbouring three C–C stretch modes.

Ionization of *anthanthrene* results in bond length changes of c, e, f, g and i bonds. Change in the charges is mainly for carbons C8, C3 and C1. The internal carbon atoms C10 and C11 have very small charge in neutral which becomes nearly zero in the cation. Theoretical vibrational data for anthanthrene are given in Table 3 and the spectra are shown in Fig. 4. Three distinct peaks for the C–H out of plane bend modes are present at 752, 807 and 887 cm^{-1}. The 752 cm^{-1} peak reflects the motion of the trio hydrogen atoms while the mode at 807 cm^{-1} is a mix of out of plane vibrations of duo and trio hydrogen atoms. 887 cm^{-1} mode corresponds to the out of plane vibrations of solo hydrogen atoms and is of highest intensity. The spectrum of the cation has similar C–H out of plane bend features as in neutral but more intense peaks are present in the 1200–1600 cm^{-1} range, which is complex and has strong modes at 1242 and 1563 cm^{-1}.

Coronene is a highly symmetric pericondensed PAH with D_{6h} point group symmetry in neutral species. Ionization results in a reduced symmetry (D_{2h}) though the structure of the molecules is not much changed. Upon ionization, major bond length changes are present in bonds c, d and f, where f is one of the inner C–C bonds. Charges of C2, C3 and C5 show maximum changes while charge of carbon C4 remains unchanged. Charge on internal carbons C6 and C7 is almost zero in both neutral and cation. Fig. 4 shows the spectra of coronene neutral and cation. In neutral the out of plane motion of the duo hydrogens contributes to 867 cm^{-1} peak. The cation spectra are rich in intense features between the range 1200 and 1550 cm^{-1} with the most intense one at 1536 cm^{-1}. Matrix isolation spectroscopy of coronene cation [32] shows the most intense feature for the C–H out of plane bend mode. This seems to be the contribution from neutral contaminants.

Table 5
Computed IR frequencies (cm^{-1}) and relative intensities for $C_{28}H_{14}$[a,b]

Neutral			Cation		
	Freq. (cm^{-1})	Rel. int.		Freq. (cm^{-1})	Rel. int.
A_u	182.6	0.03	A_u	680.3	0.08
B_u	472.1	0.03	A_u	756.3	0.04
B_u	586.4	0.04	A_u	823.5	0.14
A_u	682.7	0.16	A_u	912.9	0.18
A_u	743.9	0.09	B_u	1134.7	0.03
A_u	779.4	0.12	B_u	1160.0	0.03
A_u	809.9	0.25	B_u	1175.9	0.07
A_u	886.8	0.57	B_u	1195.1	0.06
A_u	893.4	0.15	B_u	1223.2	0.34
B_u	1057.7	0.04	B_u	1348.4	1.00
B_u	1124.8	0.03	B_u	1395.3	0.15
B_u	1186.5	0.04	B_u	1437.2	0.03
B_u	1227.9	0.05	B_u	1465.7	0.09
B_u	1307.1	0.03	B_u	1535.2	0.06
B_u	1411.1	0.04	B_u	1592.4	0.66
B_u	1416.1	0.04	B_u	3067.7	0.04
B_u	1438.3	0.10	B_u	3074.9	0.08
B_u	1483.9	0.04			
B_u	1553.4	0.04			
B_u	1563.3	0.08			
B_u	1619.3	0.07			
B_u	3018.0	0.09			
B_u	3021.4	0.21			
B_u	3025.9	0.06			
B_u	3035.5	0.18			
B_u	3046.1	0.54			
B_u	3053.4	1.00			

Max. absolute int. Neutral – 3.97 $Debye^2/amu\ Å^2$; cation – 11.75 $Debye^2/amu\ Å^2$.

[a] No experimental data available.

[b] Irreducible representations are given for each normal mode.

Table 6
Computed IR frequencies (cm^{-1}) and relative intensities for $C_{30}H_{14}$[a,b]

Neutral			Cation		
	Freq. (cm^{-1})	Rel. int.		Freq. (cm^{-1})	Rel. int.
B_{1u}	388.1	0.04	B_{1u}	388.8	0.03
B_{3u}	503.2	0.15	B_{3u}	533.9	0.11
B_{3u}	537.4	0.08	B_{3u}	756.1	0.25
B_{1u}	710.4	0.04	B_{3u}	792.7	0.17
B_{3u}	758.5	0.41	B_{3u}	924.4	0.63
B_{3u}	785.4	0.07	B_{2u}	1030.9	0.04
B_{3u}	904.8	0.90	B_{2u}	1171.1	0.04
B_{3u}	975.8	0.04	B_{2u}	1194.3	0.05
B_{2u}	1198.3	0.04	B_{2u}	1205.2	0.04
B_{1u}	1256.7	0.08	B_{1u}	1245.4	0.43
B_{2u}	1274.4	0.07	B_{2u}	1247.3	0.42
B_{1u}	1380.8	0.07	B_{2u}	1287.9	0.23
B_{1u}	1463.9	0.07	B_{2u}	1326.5	0.65
B_{2u}	1552.2	0.06	B_{2u}	1374.5	0.04
B_{1u}	1556.9	0.22	B_{1u}	1387.7	0.07
B_{1u}	1599.8	0.04	B_{1u}	1457.1	0.05
B_{2u}	1602.3	0.02	B_{2u}	1462.6	0.18
B_{2u}	3050.0	0.31	B_{1u}	1486.5	0.07
B_{2u}	3056.0	0.20	B_{2u}	1527.1	0.66
B_{2u}	3066.3	0.62	B_{1u}	1541.1	0.05
B_{1u}	3079.8	1.00	B_{1u}	1564.9	0.05
			B_{2u}	1570.9	1.00
			B_{2u}	3086.1	0.14

Max. absolute int. Neutral – 3.85 $Debye^2/amu\ Å^2$; cation – 4.99 $Debye^2/amu\ Å^2$.

[a] No experimental data available.

[b] Irreducible representations are given for each normal mode.

in the neutral as well as in the cation. The maximum change in charge is for C5. The neutral molecule has a simple spectrum (Fig. 5) with a high intensity C–H stretch

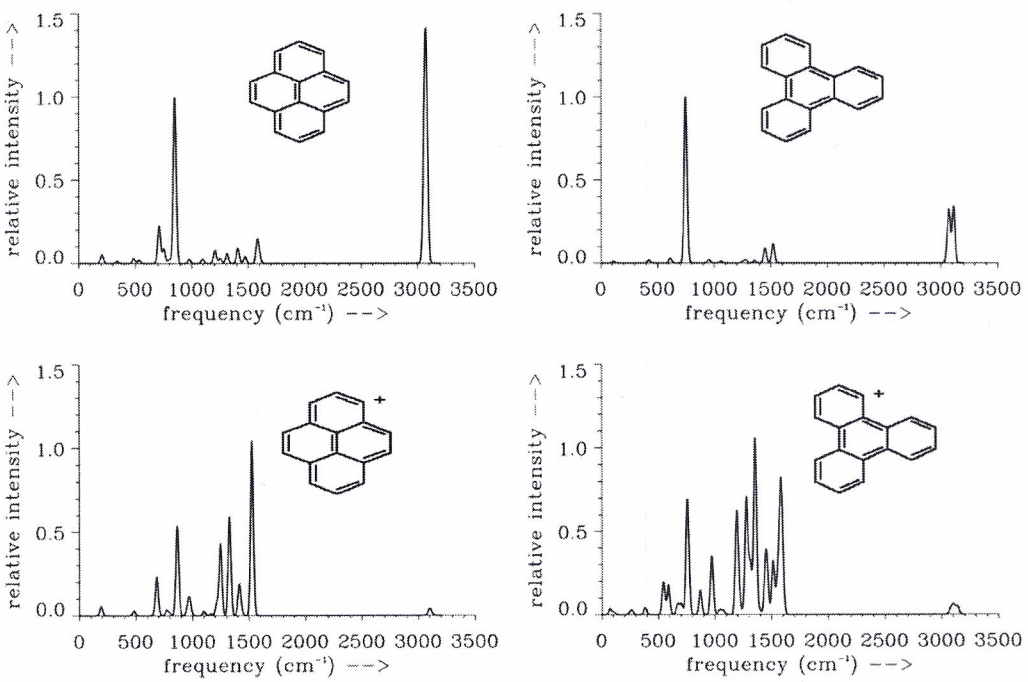

Fig. 2. Infrared spectra of pyrene and triphenylene.

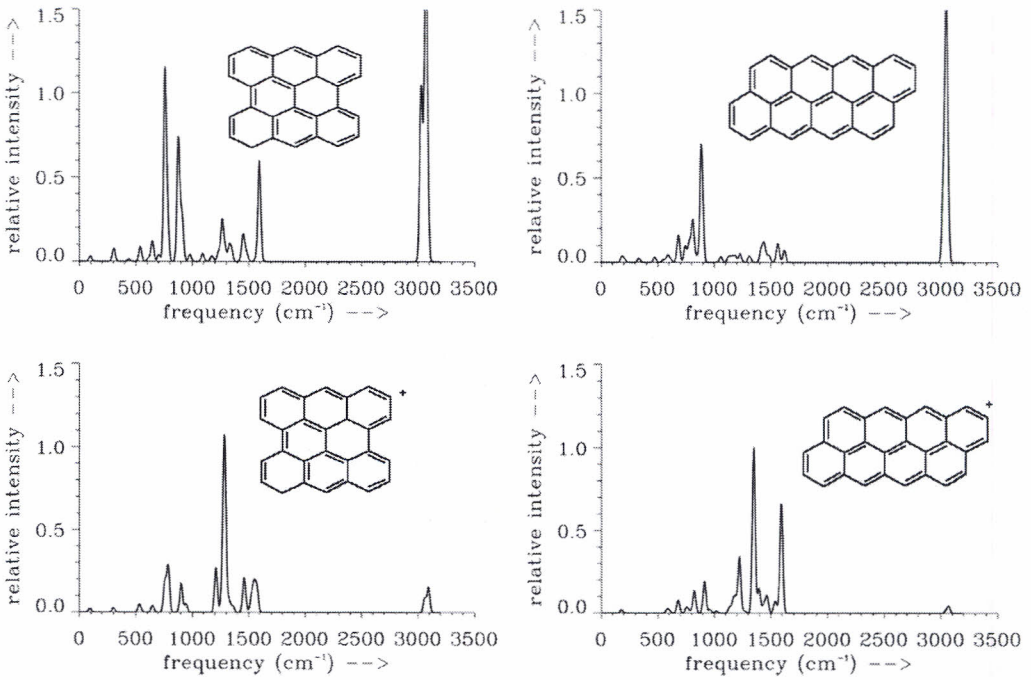

Fig. 5. Infrared spectra of bisanthene and $C_{28}H_{14}$.

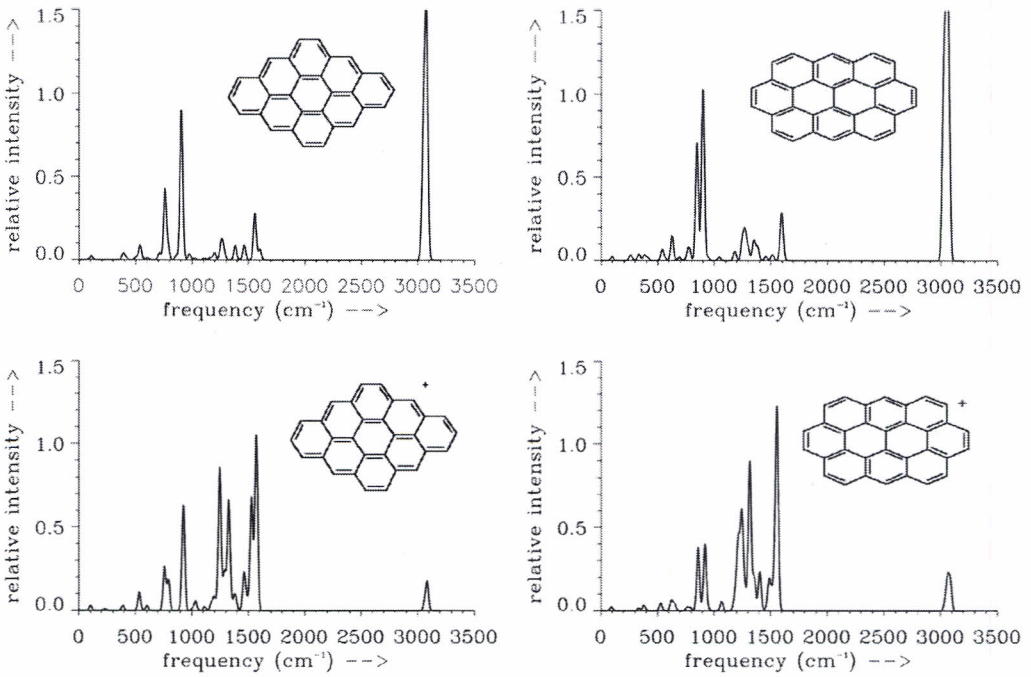

Fig. 6. Infrared spectra of $C_{30}H_{14}$ and ovalene.

molecule (Fig. 6) consists of two peaks at 905 and 759 cm^{-1} for out of plane vibrations of hydrogen atoms. The C–H stretch vibrations produce a high intensity peak at 3080 cm^{-1}. Ionization results in a more complex spectrum with several moderate intense peaks in 1200–1600 cm^{-1} range. The most intense peak lies at 1571 cm^{-1} corresponding to C–C stretch vibrations. Table 6 gives the calculated frequencies and intensities for neutral and cations.

Ionization of *ovalene* shows relatively small bond length changes compared to other pericondensed PAHs. Major

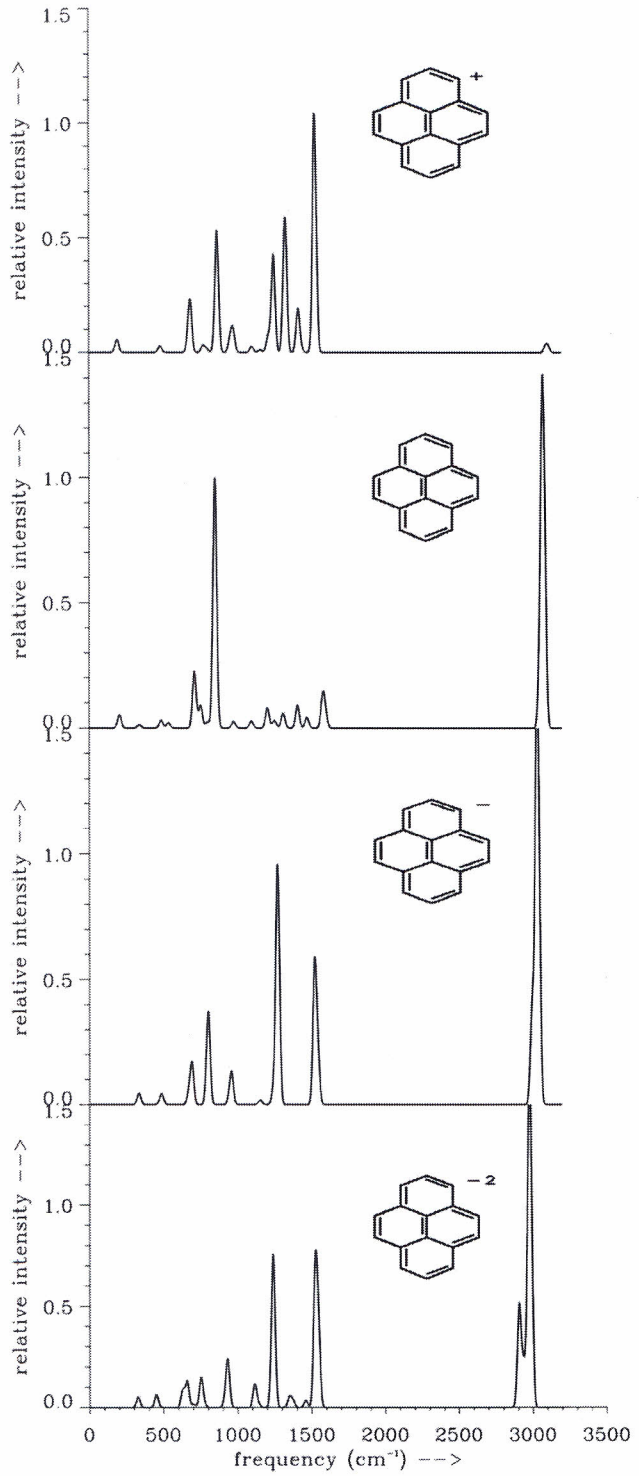

Fig. 7. Comparison of infrared spectra of various charge states of pyrene.

[48] also point to the fact that in large compact PAHs the solo C–H out of plane mode has higher intensity than other C–H out of plane modes and matches the intense AIB feature at 11.2 μm. In catacondensed and smaller PAHs [23] this is generally not the highest intensity C–H out of plane mode. The out of plane modes due to different peripheral structure around the rings lead to different peak positions. Therefore, the profile of the 11.2 μm AIB may be useful in predicting the peripheral structure and ionized state of the emitting molecules [49].

5. Astrophysical implications

The astrophysical infrared emissions depend on the excitation and internal conversion mechanisms in possible PAHs and result from transitions in higher vibrational levels. This may cause the emission features to be broader and slightly red shifted with respect to laboratory absorption bands. Laboratory emission spectra or an emission model [36] is most suitable for direct comparison with AIBs. Obtaining emission spectra in conditions close to interstellar is difficult and only a few studies have been performed [18–20,50]. An alternative is to use the results of DFT calculations as inputs for emission models [51,52].

The 3.3, 8.6 and 11.2 μm AIBs arise, respectively, from the C–H stretch, C–H in plane and C–H out of plane vibrations and the 6.2 and 7.7 μm bands from the C–C skeletal vibrations. Since, all these bands are from the PAH family of molecules, distinct relation should exist between these features. The feature variations depend on the size and charge state of PAHs that reflect the local physical conditions of the ISM. An understanding of the IR spectra of individual PAHs and their cumulative result can lead to the use of AIB observation as an astrophysical probe. Spectra of neutral PAHs only show good position match with the observed spectra while the cations provide a better match for the intensity. More cations seem to be present in star forming regions and regions having a strong UV flux while a mixture of neutrals and cations seems to be the source of AIBs in benign environments of Proto planetary-nebulae [5–7].

The prominent 3.3 μm band depends not only on the charge states of PAHs but also on the size and structure. In neutrals the intensity of this band increases with the PAH size. AIB observations and comparison with PAH spectral data has led to the conclusion that smaller PAHs give rise to this 3.3 μm band while all the other features are from comparatively larger PAHs [34,36]. While PAH cations are less likely to contribute to this mode, the intensity probably comes from neutrals and anions [53].

The C–H out of plane bend modes depend mainly on the edge structure of the emitting PAHs. The intensities and positions of various peaks for these features depend on the number of adjacent hydrogen atoms on the periphery of the PAH ring [54]. In cations these bands are blue shifted. The most prominent [48] and hence probably the most abundant is the solo hydrogen mode (11.2 μm mode). As the PAH size and compactness increases the number of solo hydrogens increases and hence the intensity of this mode.

A comparison between the co-added spectra of catacondensed PAHs [23] with the pericondensed PAHs is shown in Figs. 8 and 9. The cations of both class have intense

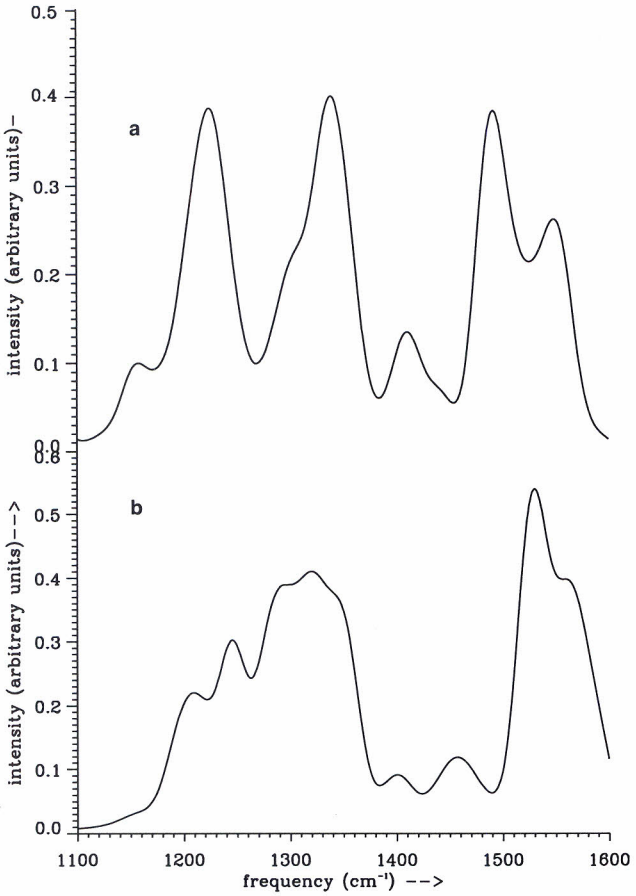

Fig. 9. Comparison of the 1100–1600 cm^{-1} region of the calculated co-added spectra (a) catcondensed PAH cations, (b) pericondensed PAH cations. The 1300 cm^{-1} feature is seen to be composed of two different peaks at 1285 and 1315 cm^{-1}.

Recently, some new infrared emission features have been detected at 6.7, 10.1, 15.8, 17.4 and 19.0 μm by the Spitzer Space Telescope [58]. Possible identifications include different modes of aromatic hydrocarbons. The study of 15–20 μm region has suggested few PAH cations to be contributing to the 19.0 μm band [59]. The 15–20 μm plateau results not only from the emissions from individual PAHs, but PAH clusters, amorphous carbon particles and other PAH related species could contribute as well. While individual PAHs seem to be responsible for the sharp features at 16.4 and 17.4 μm (610 and 575 cm^{-1}), emissions from PAH clusters could contribute to the broad structureless underlying plateau between 15 and 20 μm (670 and 500 cm^{-1}) [59]. We note that the computed spectra of pericondensed PAH cations do show a feature at 545 cm^{-1} which could correspond to the newly detected peak at 19.0 μm along with a broad plateau between 500 and 700 cm^{-1} (Fig. 8).

6. Conclusions

The charge distribution of small to medium sized pericondensed PAHs in neutral and cationic forms has been studied. The intensity changes in case of PAH ions are discussed and related to the changes occurring in the charge distribution. The charge on the hydrogen atoms has an inverse relation with C–H stretch intensity. As the positive charge on the hydrogen atom increases, the C–H stretch intensity is highly reduced and vice versa. The C–C stretch and C–H in plane bend mode intensities in the cations increase and mostly it is the change in charge of outer carbon atoms that seem to be responsible. The charge changes upon ionization of PAHs produce high intensities in the 1100–1600 cm^{-1} region for both cations and anions. This indicates that the neutral charge distribution is unique and any departure from it increases the intensity of these modes.

The charge change may be induced by ionization, by substitution, by hetero-atom addition or any other structural change.

The spectra of studied pericondensed PAHs are largely independent of the size and structure of molecules except for a few small variations. The variation in spectra in relation to size may be better understood by a study of much larger PAHs and may further help in narrowing down the possible PAHs inhabiting the ISM. Pericondensed PAHs give a better correlation with the AIBs and the band shifts and intensity variations indicate towards the possibility of larger species in the ISM. For the 7.7 μm AIB, the composite spectra of studied pericondensed PAH cations show position and profile similarity with observed A′ profile in objects having star formation activity. The IR information of a large number of PAHs in various charged states shall be useful in modelling the complete AIB spectrum in different environments. This shall help in quantifying the amount of UV flux present in the astrophysical regions and thus lead to a better understanding of the astrophysical object.

Acknowledgements

The authors acknowledge the use of computational and library facilities at Inter University Centre for Astronomy and Astrophysics, Pune. A.P. acknowledges receipt of fellowship from University Grants Commission, New Delhi. The insightful comments and suggestions of the referees are thankfully acknowledged.

References

[1] M. Cohen, A.G.G.M. Tielens, J.D. Bregman, F.C. Witteborn, D.M. Rank, L.J. Allamandola, D. Wooden, M. de Muizon, Astrophys. J. 341 (1989) 246.
[2] T.R. Geballe, A.G.G.M. Tielens, L.J. Allamandola, A. Moorhouse, P.W.J.L. Brand, Astrophys. J. 341 (1989) 278.
[3] J.D. Bregman, L.J. Allamandola, A.G.G.M. Tielens, T.R. Geballe, F.C. Witteborn, Astrophys. J. 344 (1989) 791.
[4] First ISO Results, Astron. Astrophys. 315 (1996) L26.
[5] L.J. Allamandola, D.M. Hudgins, S.A. Sandford, Astrophys. J. 511 (1999) L115.
[6] E. Peeters, L.J. Allamandola, D.M. Hudgins, S. Hony, A.G.G.M. Tielens, in: A.N. Witt, G.C. Clayton, B.T. Draine (Eds.), ASP